# Chapter 5
# Flux-Flow Oscillator (FFO) Made with the Fluxon Cloning Circuits

H. Farhan-Hassan, D. R. Gulevich, P. N. Dmitriev, V. P. Koshelets,
F. V. Kusmartsev

**Abstract** In present paper we have developed a new device, Flux-Flow Oscillator
(FFO) where flux cloning phenomena have been demonstrated. Such FFO made
with the use of flux cloning circuit can in principle operate even without magnetic
field, that is in a very different manner than conventional FFO [1] developed nowa-
days for practical applications [2, 3]. We have designed such a novel device and
build it up with the use of the long Josephson T-shaped junction of a linear overlap
geometry made up with Nb-AlO$_x$-Nb technology. We have theoretically described
the properties of such a device and the dynamics of vortices there. These theoretical
studies have been performed in the framework of a sine-Gordon model, which in-
cludes surface losses. Finally we have tested the device experimentally and demon-
strated that the flux cloning can lead to a strong coherent terahertz radiation. There
the shape of the spectral lines and the current-voltage characteristics have been also
measured.

H. Farhan-Hassan,
Department of Physics, King Abdulaziz University, Jeddah, Kingdom of Saudi Arabia,
P.O. Box 80203, Jeddah 21589, e-mail: hfarhan@kau.edu.sa
and
Loughborough University, LE11 3TU, UK

D. R. Gulevich, F. V. Kusmartsev
Loughborough University, LE11 3TU, UK, e-mail: F.Kusmartsev@lboro.ac.uk

P. N. Dmitriev, V. P. Koshelets
Kotel'nikov Institute of Radio Engineering and Electronics, Russian Academy of Science,
Moscow 125009, Russia, e-mail: valery@hitech.cplire.ru

## 5.1 Introduction

Vortices, tornados and hurricanes, like Katrina, may arise suddenly anywhere. Their prediction has grave importance for our life. The vortex nucleation has been most studied in superconductors. A common belief written in all textbooks [4] is that a single vortex cannot be nucleated inside a superconductor. It may only penetrate from the border or be created in a pair together with anti-vortex. This fact follows from the fundamental law of the vorticity conservation [4]. However for multi-connected weak superconductors (Josephson junction, JJ), there may arise a fluxon cloning, the phenomenon predicted theoretically in the Refs. [5, 6]. In general, the fluxon cloning circuits provide the producing fluxon without applied magnetic field. It is worth noting that there are many interesting configurations for a long Josephson junction such as overlap, inline and annular geometries. However, the inline and annular structures are not suitable for application as flux flow oscillators (FFO) [7], therefore previous studies have used only overlap structure as FFOs operate by applying external magnetic field. In this structure, there arise Fiske resonances which are associated with strong emission of electromagnetic radiation. Recently, it was shown that the cloned vortices may be ordered to form a train of fluxon, which is eventually operating as a flux flow oscillator created without external magnetic field for annular geometry by means of T-junction [8]. In this paper we will confine our attention to study theoretically and experimentally how a fluxons cloning circuits can be used as a FFO operating without external magnetic field from linear overlap geometry.

## 5.2 Vortex Fission Phenomena

T-shaped Josephson junction is one kind of the fluxon cloning circuits, which is an additional LJJ connected to the center of main LJJ [9]. First we consider a long T-shaped Josephson junction (presented in green colour on the Fig. 5.1(a) subjected to external magnetic field. According to [5, 6] each time when the vortex is passing the T-junction the vortex cloning arises and the new cloned vortex moves along the transverse branch of the T-junction (additional LJJ, see Fig. 5.1). The new phenomenon has been observed in numerical experiments. A single vortex propagates from the left side of the T-junction and finishes with a two-vortex state. The "baby" vortex is nucleated at the moment when a "mother" vortex passes the branching T-shaped junction. In order to give birth to a new vortex, the "mother" vortex, in main LJJ, must have enough kinetic energy. The part of this energy the "mother" vortex loses at the T-junction to generate the "baby" vortex.

   The original vortex line (denoted by 1 in the Fig. 5.1(a)) lying in the plane of the junction moves towards the T-junction. The superconducting contour around the vortex covers a single flux quantum or single vorticity. When approaching
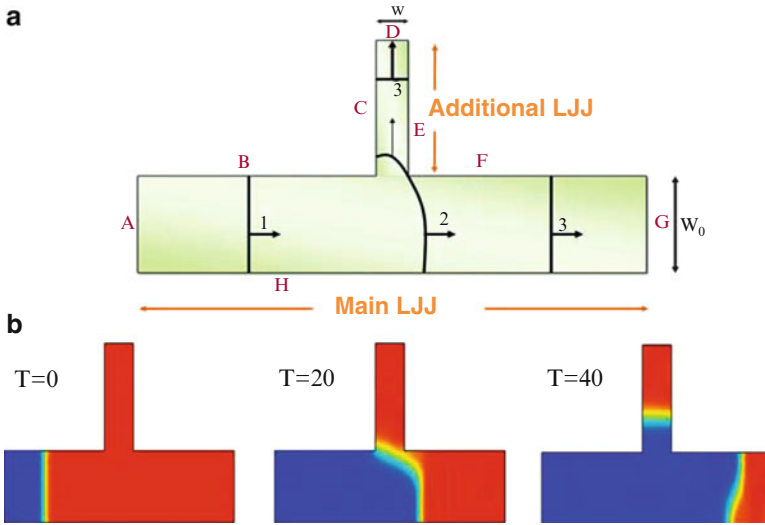
**Fig. 5.1** (Colour online) (a) A schematic picture of the vortex positions in the T-shape Josephson junction (presented in the bold lines) during the vortex nucleation process. The thin arrows indicate the direction of the vortex motion. The vortex state before nucleation is denoted by 1; the moment of nucleation is denoted by 2; the vortex state after the nucleation is denoted by 3. Widths of main and additional branches of the T-junction are $W_0$ and $W$, respectively. (b) Division of the vortex moving with velocity higher than the critical. Widths of the main and additional branches of the T-junction are $W_0 = 10$ and $W = 5\ \lambda$ respectively, where $\lambda_J$ is a Josephson length. The blue and red colours are two equivalent states of a superconductor without vortices

the T-junction the vortex is stretching and bending and its length increases. At the T-junction the vortex length is maximal, see the curved line 2 in the Fig. 5.1(a). This state is associated with the vortex nucleation barrier. At this moment the bent vortex line touches the right corner of the T-junction and the new "baby" vortex is nucleated. This nucleation happens by the corner cutting a piece from the bent ("pregnant") "mother" vortex, see the Fig. 5.1(a). As the result the original mother vortex of the enlarged length is split into two pieces of a smaller length. After the vortex division the length of the mother vortex returns to the original size $W_0$, while the size of the nucleated vortex is adapted to the width of the second branch of the junction W (see, the state 3, presented in Fig. 5.1(a) on the additional Josephson transmission line (AJTL)). The dynamics of the Josephson vortex can be traced on the colour plots (Fig. 5.1(b)), where the snapshots for the vortex positions are presented at different time intervals t. The vortex can be seen there as a green-yellow stripe, while the superconducting states without vortices are the blue and red colours. This effect is used to build up a flux flow oscillator (FFO) which can operate without magnetic field.

## 5.3 Theoretical Studying of FFOs with Fluxons Cloning Circuits

Before proceeding to the FFO from a vortex fission by using a T-junction, we
will briefly introduce the conventional FFO in long Josephson junctions [10–12].
Figure 5.2 shows schematically the junction geometries used in the FFO. A standard
overlap junction, in which the bias current is introduced in the direction perpendic-
ular to the long dimension of the junction, is shown in Fig. 5.2(a) and (b). The FFO
requires an external magnetic field, which acts through the boundaries and breaks
the symmetry of the junction. The FFO then corresponds to the continuous injection
of fluxons from one edge of the junction and their annihilation at the other bound-
ary [13]. In a Josephson FFO, when an external magnetic field is applied in plane to
the junction, the field penetrates into the junction in the form of Josephson fluxons
(solitons). In addition, they are propagated across the junction under the influence
of the bias current. Ideally, if the bias current is appropriated, a Lorentz force will
drive fluxons moving along the junction. Otherwise, fluxons are static [14,15]. Then
they are annihilated at the other edge. At this edge, when fluxons reach the junction
edge each fluxon radiates electromagnetic waves (terahertz radiation) [16–20]. The
frequency f of the radiation emitted by a moving fluxon chain is $f = V/\Phi_0$, where
$V$ is a dc voltage induced by the fluxon motion, see Fig. 5.7(a) [12, 13, 21–24].

Fluxon dynamical states in the overlap geometry are described by a
two-dimensional perturbed sine-Gordon equation model, when both external cur-
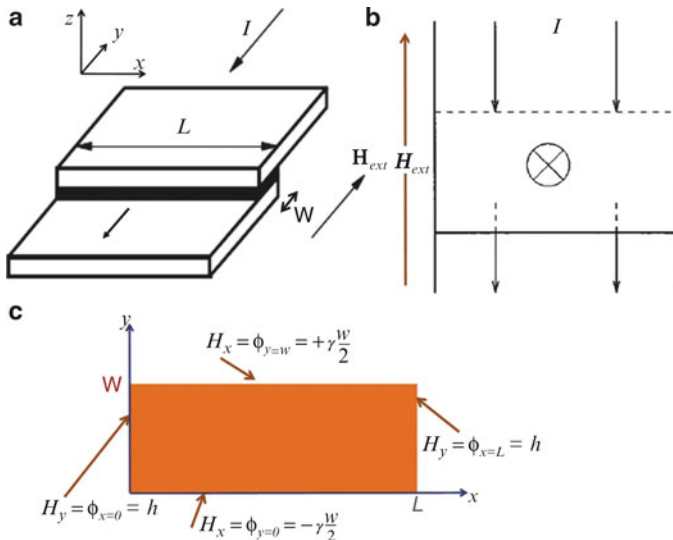rent and magnetic field are applied, where the magnetic field and the external



**Fig. 5.2** (a) Josephson tunnel junction of overlap type. (b) Schematic diagram top of the overlap
LJJ. The current from the upper electrode goes through the junction and comes in the lower elec-
trode. (c) Overlap boundary conditions for the 2D sine-Gordon equation. The magnetic field, bias
current and all lengths are dimensionless

current enter as a boundary condition on a perturbed sine-Gordon equation (PSGE) [4, 15, 23–26]

$$\phi_{xx} + \phi_{yy} - \phi_{tt} - sin(\phi) = \alpha\phi_t \tag{5.1}$$

Here, subscripts $x$ and $y$ and $t$ denote differentiation with respect to normalized space and time, respectively. Parameter $\alpha$ is a dissipation coefficient (the damping), which is assumed to be a real number with $\alpha \geq 0$. In an overlap structure, as shown in Fig. 5.2, the normalized total length and width of junctions are L and W along the x and y axes, respectively. The general boundary conditions for PSGE have the form

$$n.\nabla\phi_{|_{\partial\Omega}} = n.[z \times (H_e + H_I)]_{|_{\partial\Omega}} \tag{5.2}$$

where $n$ is the outward normal to the boundary $\partial\Omega$ of the junction region $\Omega$, $H_e$ is an external dimensionless magnetic field and $H_I$ is the magnetic field caused by a current passing through the junction. When an external magnetic field Hext is applied to the plane of the junction parallel to the barrier and perpendicular to the length of junction, the boundary conditions may be written [4, 13, 23–29] in form

$$H_y = \frac{d\phi}{dx}_{|_{x=0,L}} = h \tag{5.3}$$

$$H_x = \frac{d\phi}{dy}_{|_{y=0,W}} = \mp\gamma\frac{W}{2} \tag{5.4}$$

where $h = H_{ext}/(J_c\lambda_J)$ denotes the normalized measure of the external magnetic field and $\gamma$ is the normalized measure of the y-component of the external current injected at the junction boundary, see Fig. 5.2(b) and (c).

Now, let us consider a fluxon cloning circuits by means of T-shaped Josephson junction as shown in Fig. 5.1. The boundaries A, D and G in Fig. 5.1 convert to the sharp ends which are added to avoid reflecting of vortices from the ends of the junction as shown in Figs. 5.3–5.5. The magnetic vortices only penetrate from boundaries A and G of the main LJJ. In these circuits, a main LJJ branch (width $W_0$) is a main FFO junction (conventional FFO junction) and an additional LJJ branch (width $W$) is a 'side' FFO junction. In addition, all part of a Josephson junction oscillate with the same frequency (i.e. the mean voltage in all parts of a Josephson junction is the same). When the applied external magnetic field exceeds the critical value, $h_{min}$, which is required for the fluxon to penetrate inside the junction in the absence of a bias current, the magnetic flux begins to be entered through both boundaries A and G of main FFO and pushed into the junction in the form of separated vortices. These vortices are pinned on the inhomogeneity of the junction (see Fig. 5.3(a)). As the field increases, see Fig. 5.3(b), new vortices penetrate through the boundaries and push the previous ones towards the T-junction [30]. At the T-junction, vortices are stuck because they do not have enough energy to overcome the barrier energy of the T-junction. At a high value of h, although fluxons may flow fast into the junction, they still cannot fission, see Fig. 5.3.

Furthermore, fluxons injected into the main FFO junction boundaries by an external magnetic field are accelerated into the interior of the junction by an externally applied bias current. If the current exceeds its critical value, the flux into the junction will necessarily begin to flow [15, 21] and fission at T-junction. With $\gamma > 0$, the critical value of the magnetic field is reduced [15, 31]. When the combination of $\eta$ and $\gamma$ is appropriately above threshold values, fluxons may have enough kinetic energy to fission at the T-junction. First, fluxons penetrate the main FFO junction from both boundaries A and G, as shown in Fig. 5.4. These fluxons, which are propagated in the junction, are controlled by two forces: the driving force, which acts on vortices in the $-x$ direction and the magnetic force, which acts in the $x$ direction on entering vortices from boundary A and in the $-x$ direction on entering vortices from boundary G. Second, at a low bias current, the effect of a Lorentz force is weak. Vortices penetrate the junction from both boundaries A and G and accelerated toward the other opposite side from a penetration (boundaries G and A, respectively (see Fig. 5.4(a)). Nevertheless, the fluxons' motion from boundary G is faster than that from boundary A. Therefore, the number of fluxons on the right side is higher than on the left side. In addition, the vortices on the left side may be pinned in the junction (Fig. 5.4(a) and (b)), depending on the strength of the magnetic field. Meanwhile, the fluxons on the right side begin to fission very slowly by the T-junction and move in main and additional LJJ toward boundaries A and D, respectively. Then, the cloned fluxons, which moved in main FFO, begin propagating to the right and push the vortices which are pinned in the left side of the junction. After a long time, therefore, all fluxons in main FFO move to the left. Eventually, as the value of $\gamma$ is increased still further, the fluxons may start to flow through the main FFO junction only from boundary G (from right to left) because of a Lorentz force (see Fig. 5.4(c)). At the T-junction, the first fluxon begins splitting into two vortices in main FFO and additional FFO. Then, they continue propagating to the junction boundaries A and D. The same process happens with the second, third and following fluxons. Therefore, the train of fluxons flows into additional LJJ, which may be used as an FFO operating without an applied external magnetic field.

## 5.4 Numerical Results

We have performed the numerical experiments with the use of the finite element program package COMSOL Multiphysics [32]. The time-dependent two-dimensional sine-Gordon equation [1] has been solved using a mesh consisting of 5908 elements. Using a time-dependent solver, it demonstrates a succession of penetration of magnetic flux, soliton moving and vortices fission. The dynamics of the magnetic flux during change time can be traced on the colour plots, for example Figs. 5.3–5.5. The colour scale represents the distribution of the magnetic field as the dark blue colour represents the minimum value and red colour represents the maximum (see the colour scale in Figs. 5.3–5.5). The snapshots for the magnetic vortex positions

are presented at different time intervals t. The boundary conditions of the junction, Eq. 5.2, are represented in program as

$$n.\nabla\phi_{|B,F,H} = -\gamma\frac{W_0}{2} \tag{5.5}$$

$$n.\nabla\phi_{|C,E} = -\gamma\frac{W}{2} \tag{5.6}$$

$$n.\nabla\phi_{|A,G} = \pm h \tag{5.7}$$

$$n.\nabla\phi_{|D} = 0 \tag{5.8}$$

Long Josephson Nb-AlO$_x$-Nb junctions with overlap geometry are used as FFOs with splitting circuits. These circuits are diminutions as $L = 400\,\mu m$ and $W_0 = 16\,\mu m$ for main FFO and $L = 200\,\mu m$ and $W = 8\,\mu m$ for "side" FFO. All lengths are represented in program in units of the Josephson penetration depth. $\lambda_J = 8\,\mu m$ [33]. The damping parameter was used 0.1 and magnetic field and electric current bias were chosen qualitatively.

First of all, we have studied the dynamics of vortices in flux cloning circuits at zero driving current and at different values of the magnetic field, which were applied to boundaries A and G of the main FFO. Figure 5.3 shows examples of the penetration of magnetic flux into the junction at different values of magnetic field. It can be detected on the colour plots in Fig. 5.3 at $h = 1.4$, 2, and 3. At $h = 1.4$, only a single fluxon can enter but it stops after moving a short distance. When the magnetic field is increased, see Fig. 5.3(b) and (c), one may see that, although the magnetic field is high, the vortices cannot clone at the T-junction. In Fig. 5.3(b), $h = 2$, many fluxons can pass through the junction at T = 40, but these vortices are bonded when they approach the T-junction. In case $h = 3$, although the concentration of the fluxons increases, they are trapped by the T-junction, see Fig. 5.3(c). In addition, it is clear the spacing between the moving fluxons is inversely proportional to $h$ (see Fig. 5.3(b) and (c)).

Further, we have investigated the efficiency of 'side' FFO in flux cloning circuits when the external bias current and magnetic field are applied to main FFO. First, we fixed the external magnetic field, for example $h = 2$. The dynamics of magnetic flux at different bias currents can be traced on the colour plots in Fig. 5.4. At a low bias current, $\gamma = 0.04$, fluxons penetrating from the right side of the T-junction are more numerous than those from the left side (see Fig. 5.4(a) at T = 40). In addition, the vortices on the right side move at high speed, whereas vortices on the left side move slowly. The motion of these vortices, on the left side, gradually decreases when they approach the T-junction. Sometimes they may nearly hold inside the junction, as shown in Fig. 5.4(a) at T = 70 (the vortices are not pinned if $h = 3$ as shown in Fig. 5.5). On the right side of the figure T-junction, the fluxons approaching the T-junction start fission slowly by the T-junction. Therefore, fluxons tend to concentrate and slow down before the T-junction. Then, the fluxons that have split
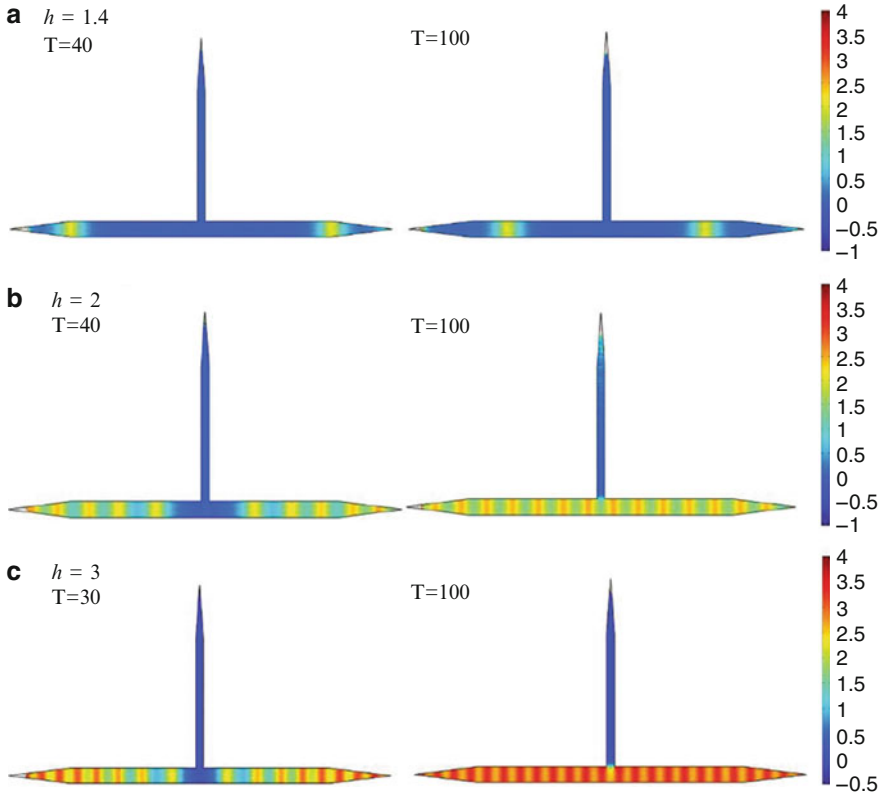
**Fig. 5.3** (Colour online) Numerical simulations for the penetration of magnetic flux into junction without applied bias current. (a) At $h = 1.4$, only one vortex can enter from each boundaries A and G. They penetrate a small distance into the junction and then are pinned. (b) At $h = 2$, many vortices can pass through the junction. At T-junctions, these vortices are bonded and are not cloned. (c) At $h = 3$, the penetrated vortices are moved fast. The concentration of fluxons in the junction also increases. Vortex fission does still not occur. The colour scale represents the distribution of the magnetic field from $-0.5$ to 4

accelerate and propagate in both main LJJ and additional LJJ toward the ends of the LJJ. On the left side of the T-junction, vortices (in the main FFO) accelerate after passing the T-junction and push the pinned fluxons to move in $-x$ direction. As a result, after a long time, all fluxons in the main FFO move from right to left. When the bias current increases, the speed of vortices on the right side increases; however, the speed of vortices on the left side reduces. For instance, if $\gamma = 0.08$, the dynamics of the magnetic vortices are exactly the same as if $\gamma = 0.04$ but succession divisions require less time, as shown in Fig. 5.4(a) and (b). In addition, the distance of the propagated fluxons from the left side is decreased (see Fig. 5.4(a) at T $= 70$ and Fig. 5.4(b) at T $= 50$).
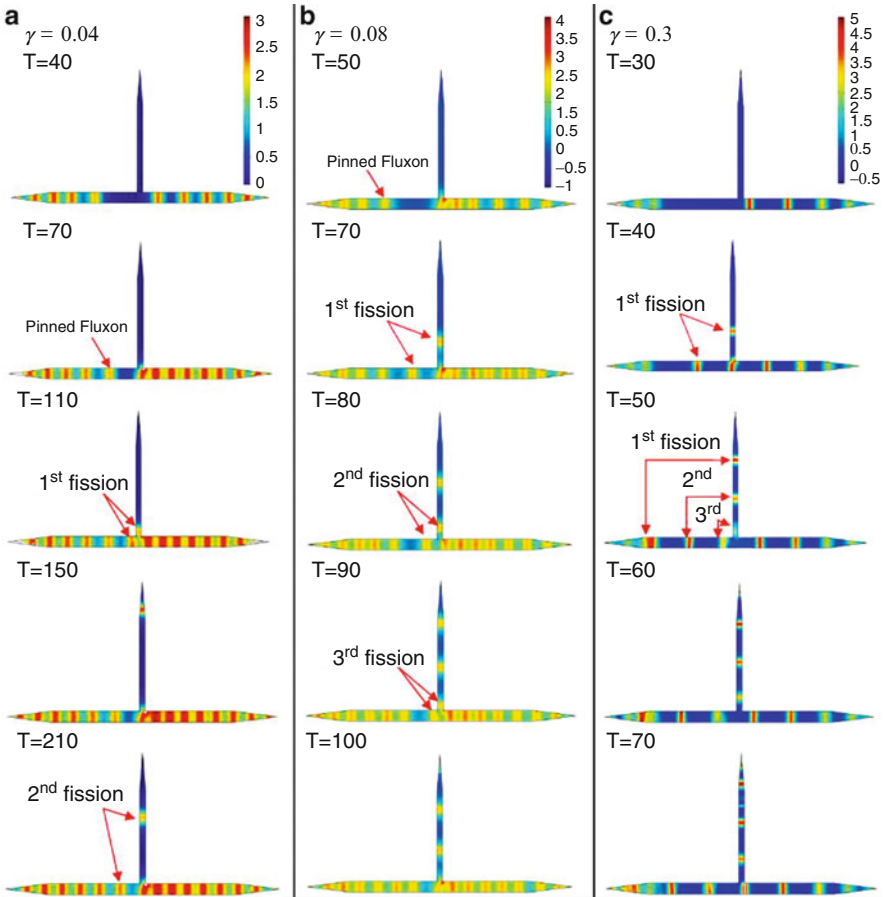
**Fig. 5.4** (Colour online) Numerical simulations for penetration of magnetic flux into junction when variable bias current at $h = 2$. (a) At $\gamma = 0.04$, the most vortices are entering from the right side of the main FFO. On left side of the main FFO, they struggle to approach the T-junction. Then, they are pushed to right by cloned vortices, which enter from T-junction. Vortex fission occurs slowly. (b) At $\gamma = 0.08$, the acceleration of vortices from the right side increases while the vortices from the left side slowdowns. The flowing of vortices and their fission take less time. (c) At $\gamma = 0.3$, vortices in main FFO flow from the right to the left. There are quickly in vortex fission. The colour scale represents the distribution of the magnetic field

At a high bias current of $\gamma = 0.3$, the magnetic fluxes fluently flow from right to left in main FFO. In addition, when vortices approach the T-junction, they can split effortlessly (see Fig. 5.4(c)). From Fig. 5.4 one may see that the time required for sequencing divisions is inversely proportional to the value of bias current. In case $\gamma = 0.3$, a series of cloned fluxons occurs quickly. Therefore, the chain of fluxons can produce in an additional LJJ. In this case, the additional LJJ can be used as a FFO operating without applying an external magnetic field to this stripe.
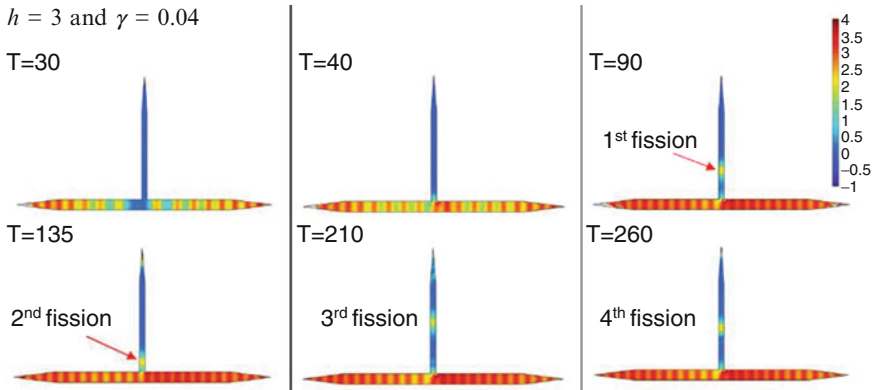
$h = 3$ and $\gamma = 0.04$



**Fig. 5.5** (Colour online) Numerical simulations of magnetic flux penetration into the junction when $h = 3$ and $\gamma = 0.04$. In main FFO, fast vortices enter from each boundaries A and G and move toward T-junction. Vortices on the left side are continued to move toward T-junction without stopping (no pinning is observed). Because of speedy vortices originated from the right side, they pass through T-junction and continue moving to the left with pushing vortices on left side and moving to left direction. Succession divisions are a bit faster than in the case $h = 2$ in Fig. 5.4(a). The colour scale represents the distribution of the magnetic field

## 5.5 Experimental Results

The described above flux cloning circuits have been studied experimentally. A prepared sample made of additional LJJ (width $8\,\mu m$, length $200\,\mu m$), which is connected to the main LJJ (width $16\,\mu m$, length $400\,\mu m$). IVCs of the FFO measured are presented in Fig. 5.6. The different curves correspond to different values of magnetic field. The colour of lines correspond to radiation coming from additional LJJ. From this figure, it is clear that because of presence of the splitting point there is non-zero return current on the FFO IV curves even at large magnetic field. Presumably it means that fluxons are trapped at the inhomogeneity at the T-junction and considerable current is required to move fluxon in the presence of the splitting point. In addition, important feature of the most FFO IVCs is almost complete absence of the Fiske steps as we predict. There are only such steps arise only at high magnetic fields, when the density of fluxons is large and they are associated with resonance created on additional LJJ.

It's possible to detect emitted radiation and its power. However, only at some very specific frequency range a very narrow-band radiation has been measured (see Fig. 5.7). The frequency of the FFO is determined by its voltage according to Josephson relation. The measured peak behaves as regular Josephson radiation peaks (checked by measurements of the frequency shift at small variation of the FFO voltage), (see Fig. 5.7). Often higher harmonics of emitted radiation can be detected at biasing on these steps. Spacing of these steps (about $50\,\mu V$) is close
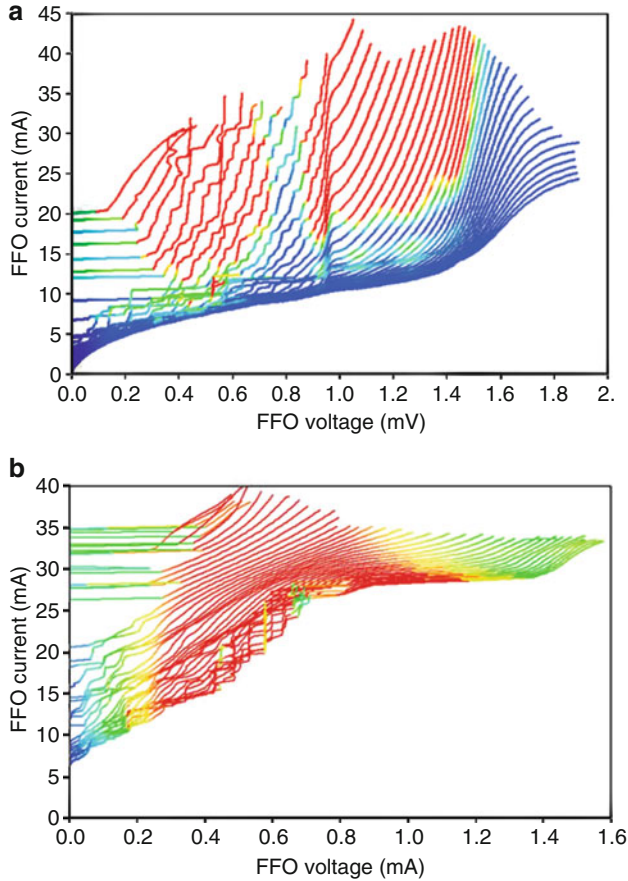
**Fig. 5.6** (Colour online) (a) Experimental measured IVCs for conventional FFO at different magnetic fields created by current applied to integrated control line. (b) IVCs of the FFO with flux cloning circuits at different magnetic fields created by current applied

enough to expected distance between Fiske steps for 200 μm FFO. No narrow-band radiation was detected at other FFO biasing except these steps, only at high voltages very wide peaks were measured (see Fig. 5.7(b)).

## 5.6 Conclusions

In the present work we have developed a new device which we call Flux Flow Oscillator with Cloning Circuit. This device may serve as an effective source of terahertz radiation. The coherent radiation is due to a Fiske resonance which is formed by
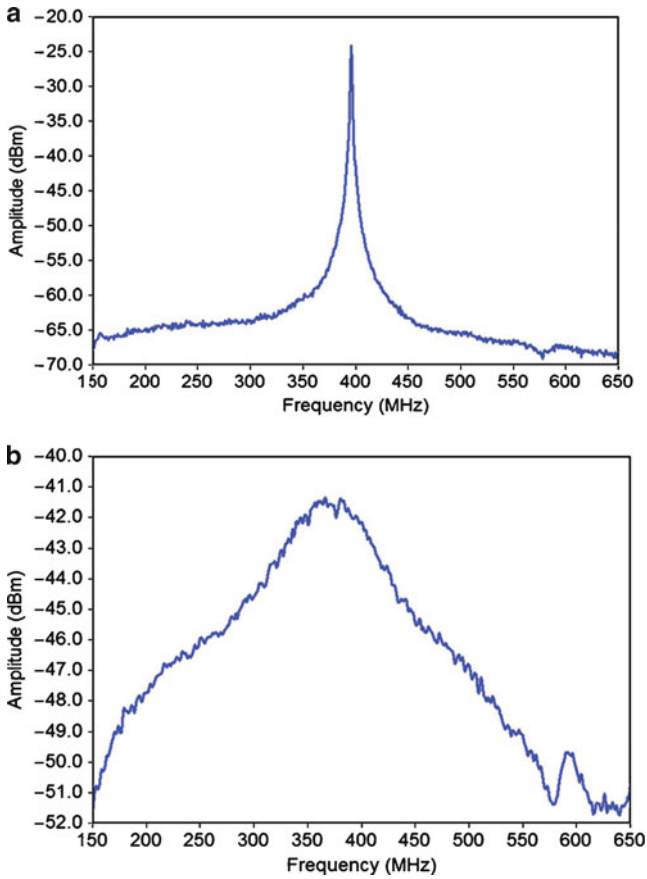
**Fig. 5.7** FFO spectra associated with radiation emitted by additional LJJ. (a) Frequency – 216 GHz, linewidth – 1.4 MHz. (b) FFO frequency – 716 GHz, linewidth – 130 MHz

a train of fluxons cloned in the T-shaped Josephson junction. Therewith, for the first time we found experimentally and described theoretically that indeed the vortex cloning does exist and, as a result, many single Josephson vortices can be born inside a superconductor and for a dense vortex train even without an application of magnetic field despite the common belief [1]. We found that when these cloned vortices are ordered in a line to form a train which period is commensurate with the size of the additional Josephson transmission line (AJTL) there arise a strong Fiske resonance. Such resonance is, in turn, accompanied by terahertz radiation intensively emitted along the AJTL. Thus such a system eventually forms a flux flow oscillator created without external magnetic field. We have also identified a series of resonance frequencies where such trains from cloned vortices generate a strong coherent terahertz radiation. We have measured the shape of these spectral lines and found that they are very narrow and the device can serve as FFO in system where application of magnetic field is limited.

# References

[1] T. Nagatsuma, K. Enpuku, F. Irie, and K. Yoshida, J. Appl. Phys., 54, 3302, (1983), see also Pt. II: J. Appl. Phys. 56 3284 (1984); Pt. III, J. Appl. Phys., 58 441 (1985); Pt. IV, J. Appl. Phys. 63. 1130 (1988)

[2] V. P. Koshelets et al, IEEE Trans. on Applied Superconductivity, 5, 3057, 1995.

[3] G. de Lange, et al, Supercond. Sci. Technol. vol. 23, 045016, (2010).

[4] A. Barone and G. Paterno, Physics and Applications of the Josephson Effect, John Wiley and Sons, Inc. (1982).

[5] D. .R.Gulevich, F.V. Kusmartsev, Phys Rev. Lett., 97, 017004, 2006.

[6] D. .R.Gulevich, F.V. Kusmartsev, Supercond. Sci. Technol. 20, S60-S67, 2007.

[7] M. Jaworski, Supercond. Sci. Technol., 21, 065016, 2008.

[8] D. R. Gulevich, F.V. Kusmartsev, S. Savel'ev, V.A. Yampol'skii, F. Nori, Phys. Rev. Lett. 101, 127002, 2008.

[9] H. S. Newman, K. L. Davis , Journal of Applied Physics, 53, 7026-7032, 1982.

[10] M. Jaworski, Supercond. Sci. Technol., 21, 065016, 2008.

[11] N. Thyssen, A. V. Ustinov, H. Kohlstedt, Journal of Low Temperature Physics, 106, 201-206, 2006.

[12] J. Mygind, N.F. Pedersen, Microwave Superconductivity, H. Weinstock and M. Nisenoff (ed), 1999.

[13] N. Pedersen, A. V Ustinov, Supercond. Sci. Technol., 8, 389-401, 1995.

[14] H. H. Sung, S. Y. Yang, H. E. Homg and H. C. Yang, IEEE TRANS. ON APPL.SUPER., 9, 3937-3940, 1999.

[15] R. D. Parmentier, The New Superconducting Electronics, 2 ed H Weinstock and R W Ralston (Dordrecht: Kluwer) 1993.

[16] R. G. Mints, I. B. Snapiro, Phys. Rev. B, 52, 9692, 1995.

[17] L. N. Bulaevskii, A. E. Koshelev, Journal of superconductivity and novel magnetism, 19, 349, 2006.

[18] V. V. Kurin and A. V. Yulin, Phys. Rev. B 55, 11659, 1997.

[19] A. A. Abdumalikov, M. V. Fistul, and A. V. Ustinov, Phys. Rev. B 72, 144526, 2005.

[20] E. Goldobin, A. Wallraff, A. V. Ustinov, Journal of Law Temp. phys., 119, 589, 2000.

[21] A. A.Golubov, B.A.Malomed3 and A. V. Ustinov, Proceedings of the 21st International Conference on Low Temperature Physics, Czechoslovak Journal of Physics, 46, 573-574, 1996.

[22] A. P Betenev, V. V. Kurin, Phys.Rev. B, 56, 7855-7857, 1997.

[23] J. Caputo, N. Flytzanis, Y. Gaididei, and E. Vavalis, Phys. Rev., 54, 2092-2021, 1996.

[24] A. V. Ustinov, Long Josephson Junctions and Stacks

[25] J. C. Eilbeck, P. S. Lomdahl, O. H. Olsen, J. Appl. Phys. 57 (3), 861-866, 1985.

[26] P. S. Lomdahl, O. H. Olsen, J. C. Eilbeck, J. Appl. Phys. 57 (3), 997-999, 1984.

[27] N. F. Pederson, Solitons in Josephson transmission lines, in Solitons, S. E. Trullinger, V. E. Zakharov, and V. L. Prokovsky, eds., North-Holland, Amsterdam, 1986.

[28] S.G. Lachenmann, G. Filatrella, T. Doderer, J.C. Fernandez, R.P Huebener, Phys. Rev. B, 48, 22 (1993).

[29] J. C. Eilbeck, P. S. Lomdahl, O. H. Olsen, and M. R. Samuelsen, J. Appl. Phys., 57, 861, 1985.

[30] S. N. Dorogovtse, A. N. Samukhin, Euro phys. Lett., 25, 693-698, 1994.

[31] M. Cirillo, T. Doderer, S.G. Lachenmann, F. Santucci, and N. Grnbech-Jensen, Phys. Rev. B, 56, 11 889, 1997.

[32] W. B. Zimmerman, World Scientific, Singapore, 2006.

[33] V. P. Koshelets and S. V. Shitov, Supercond. Sci. Technol., 13, R53, 2000.